Imaging Characteristics of Choroid Plexuses in Presymptomatic Multiple Sclerosis

A Retrospective Study

Vito A.G. Ricigliano, MD, PhD, Céline Louapre, MD, PhD, Emilie Poirion, PhD, Annalisa Colombi, MD, Arya Yazdan Panah, MSc, Andrea Lazzarotto, MD, Emanuele Morena, MD, Elodie Martin, PhD, Michel Bottlaender, MD, PhD, Benedetta Bodini, MD, PhD, Danielle Seilhean, MD, and Bruno Stankoff, MD, PhD

Correspondence
Prof. Dr. Stankoff
bruno.stankoff@aphp.fr

Abstract

Background and Objectives
Recent imaging studies have suggested a possible involvement of the choroid plexus (CP) in multiple sclerosis (MS). Here, we investigated whether CP changes are already detectable at the earliest stage of MS, preceding symptom onset.

Methods
This study is a retrospective analysis of 27 patients with presymptomatic MS, 97 patients with clinically definite MS (CDMS), and 53 healthy controls (HCs) who underwent a cross-sectional 3T-MRI acquisition; of which, 22 MS, 19 HCs, and 1 presymptomatic MS (evaluated 8 months before conversion to CDMS) also underwent translocator protein (TSPO) ^{18}F-DPA-714 PET and were included in the analysis. CPs were manually segmented on 3D T1-weighted images for volumetric analysis. CP ^{18}F-DPA-714 uptake, reflecting inflammation, was calculated as the average standardized uptake value (SUV). Multivariable regressions adjusted for age, sex, and ventricular and brain volume were fitted to test CP volume differences between presymptomatic patients and MS or HCs. For the presymptomatic case who also had ^{18}F-DPA-714 PET, CP SUV differences with MS and HCs were assessed through Crawford-Howell tests. To provide further insight into the interpretation of ^{18}F-DPA-714-PET uptake at the CP level, a postmortem analysis of CPs in MS vs HCs was performed to characterize the cellular localization of TSPO expression.

Results
Compared with HCs, patients with presymptomatic MS had 32% larger CPs (β = 0.38, $p = 0.001$), which were not dissimilar to MS CPs ($p = 0.69$). Moreover, in the baseline scan of the presymptomatic case who later on developed MS, TSPO PET showed 33% greater CP inflammation vs HCs ($p = 0.04$), although no differences in ^{18}F-DPA-714 uptake were found in parenchymal regions vs controls. CP postmortem analysis identified a population of CD163^{+} mononuclear phagocytes expressing TSPO in MS, possibly contributing to the increased ^{18}F-DPA-714 uptake.

Discussion
We identified an imaging signature in CPs at the presymptomatic MS stage using MRI; in addition, we found an increased CP inflammation with PET in a single presymptomatic patient. These findings suggest a role of CP imaging as an early biomarker and argue for the involvement of the blood-CSF barrier dysfunction in disease development.

Glossary

BCSFB = blood-CSF barrier; **CPs** = choroid plexuses; **DVR** = distribution volume ratio; **EAE** = experimental autoimmune encephalomyelitis; **FLAIR** = fluid-attenuated inversion recovery; **HAB** = high-affinity binder; **HCs** = healthy controls; **MPRAGE** = magnetization-prepared rapid gradient echo; **MS** = multiple sclerosis; **NAWM** = normal-appearing WM; **RIS** = radiologically isolated syndrome; **ROIs** = regions of interest; **RRMS** = relapsing-remitting MS; **SUV** = standardized uptake value; **TE** = echo time; **TIV** = total intracranial volume; **TR** = repetition time; **TSPO** = translocator protein; **WM** = white matter.

Trial Registration Information

APHP-20210727144630, EudraCT-Number: 2008-004174-40; ClinicalTrials.gov: NCT02305264, NCT01651520, and NCT02319382.

Choroid plexuses (CPs) are CNS structures involved in CSF production and immunosurveillance.[1] They regulate the bidirectional exchange between the blood and the CSF, forming the so-called blood-CSF barrier (BCSFB).[2,3] Their structural and functional alterations may contribute to the pathophysiology of immune-mediated CNS diseases such as multiple sclerosis (MS). We previously described, in a study combining MRI and inflammatory PET in patients with MS vs healthy controls (HCs), that CPs have greater volume and higher translocator protein (TSPO) expression at the inflammatory phase of the disease, possibly reflecting increased macrophage/microglia infiltration.[4] We demonstrated that CP enlargement correlated with imaging metrics of parenchymal inflammation and with the relapse rate in relapsing-remitting MS (RRMS). Recently, the role of CP volumetric increase as a neuroinflammatory marker over time has been corroborated in a translational study.[5]

In the experimental autoimmune encephalomyelitis (EAE) model, CPs allow the initial lymphocytic infiltration into the CNS.[6,7] In human pathology, this early presymptomatic phase of the disease is often referred to as radiologically isolated syndrome (RIS).[8,9] This entity corresponds to patients with radiologic signs of MS without neurologic events but with a higher risk of clinical conversion for males, aged <37 years, and with cervical/thoracic spinal cord lesions and gadolinium-enhancing lesions.[10,11] Thus far, however, definite predictive imaging markers at the presymptomatic stage are lacking, and a possible involvement of CPs at this early subclinical phase of MS has never been investigated in vivo.

To this aim, we performed a 3T MRI volumetric analysis of CPs in a cohort of 27 patients with presymptomatic MS (26 RIS and 1 woman with presymptomatic MS with 2 WM lesions, one of which in a MS-typical CNS location) vs 97 patients with MS and 53 HCs. Moreover, we measured CP inflammation with TSPO ^{18}F-DPA-714 PET in 1 patient with presymptomatic MS who converted to clinically defined MS 8 months later and compared results with 22 MS and 19 HCs. Finally, we characterized the cellular localization of CP TSPO expression in the disease on postmortem samples.

Methods

Patients

Twenty-six patients fulfilling the 2009 RIS diagnostic criteria,[8] followed between September 2013 and January 2021, and validated by the RIS International Consortium, for whom MRI scans with nonenhanced 3D T1-weighted sequences were available, were retrospectively selected from our Neurology Clinics of Saint-Antoine and Pitié-Salpêtrière Hospital in Paris, France. Clinical history, CSF positivity (either high IgG index or positive oligoclonal bands),[11] conversion to MS, and follow-up duration (months) since the analyzed MRI were collected until August 2021. Consent according to the French legislation for noninterventional research was obtained from all patients (APHP-20210727144630). In addition, a 30-year-old woman with presymptomatic MS, originally included as a healthy volunteer in a protocol combining 3T-MRI and ^{18}F-DPA-714 PET for the study of innate immune cell activation in patients with MS vs HCs (ClinicalTrials.gov: NCT02305264)[12] but then classified as presymptomatic MS, was added to the studied cohort. After genotyping of the rs6971 variation of *TSPO* gene,[13] she was classified as a high-affinity binder (HAB).

A retrospective convenience series of 97 patients with MS (61 RRMS and 36 progressive MS) and 53 HCs from 4 prospective cross-sectional studies performed between 2009 and 2017 (EudraCT-Number: 2008-004174-40; ClinicalTrials.gov: NCT02305264, NCT01651520, and NCT02319382)[4,14] was used to collect MRI data. From this population, 37 patients and 28 HCs also underwent ^{18}F-DPA-714 PET at study entry (ClinicalTrials.gov: NCT02305264 and NCT02319382).[12,14] After rs6971 genotyping, 22 patients with MS and 19 HCs were classified as HAB for *TSPO* sequence variant and kept for further analysis (NCT02305264 and NCT02319382).

Standard Protocol Approvals, Registrations, and Patient Consents

Written informed consent was obtained from all participants according to the Declaration of Helsinki, and the studies were approved by the local ethic committees. Trial registration

Figure 1 Enlarged CPs in Presymptomatic MS
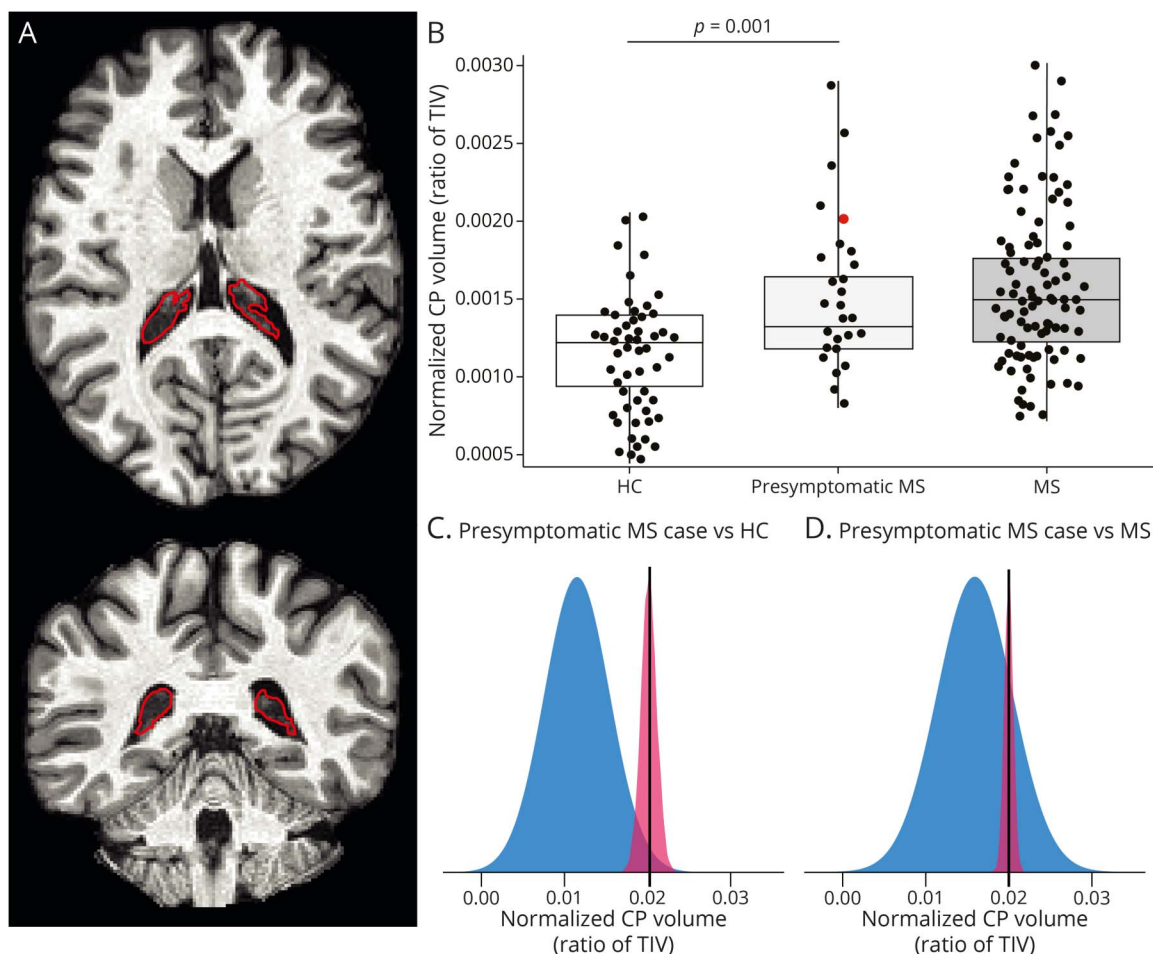
(A) Unenhanced 3D T1-weighted magnetization-prepared rapid gradient echo (MPRAGE) images showing the segmentation of the left and right CP (outlined in red) in axial (top) and coronal (bottom) planes in a patient with presymptomatic MS. (B) Box plots showing significantly higher CP volume in the whole presymptomatic MS group vs HCs and no difference compared with MS. CP volume was normalized according to TIV. Note that the dot corresponding to the volume of the presymptomatic case further examined in the PET part of this study is colored in red. Box represents the interquartile range and median, whereas whiskers represent minimum and maximum values in data. The p value corresponds to that of the multivariable linear regression model. (C–D) Graphical illustration of the distribution of normalized CP volume in HCs vs the single presymptomatic woman (C) and in MS vs the single presymptomatic woman (D) from the Crawford-Howell test. Note that the presence of a distribution for a single case value is based on the assumptions of the test performed and depends on the statistics of the reference cohort. CP = choroid plexus; HCs = healthy controls; MS = multiple sclerosis; TIV = total intracranial volume.

numbers: APHP-20210727144630, EudraCT-Number: 2008-004174-40; ClinicalTrials.gov: NCT02305264, NCT01651520, and NCT02319382.

Image Acquisitions

All patients underwent a 3T-MRI examination including the following sequences: 3D T1-weighted magnetization-prepared rapid gradient echo (3D-T1 MPRAGE), 2D turbo spin-echo T2-weighted (T2-w), and/or T2 fluid-attenuated inversion recovery (FLAIR). Sequence parameters for the research protocols were (1) 3D-T1 MPRAGE: repetition time (TR)/ echo time (TE): 2,300/2.98 ms, inversion time: 900 ms, and resolution: $1.0 \times 1.0 \times 1.1$ mm3; (2) T2-w: TR/TE: 4,100/83 ms and resolution: $0.9 \times 0.9 \times 3.0$ mm^3; and (3) FLAIR: TR/ TE: 8,880/129 ms and resolution: $0.9 \times 0.9 \times 3.0$ mm^3.

^{18}F-DPA-714 PET examinations were performed on a 3D high-resolution research tomograph (CPS Innovations, Knoxville,

TN) with a 31.2-cm transaxial and 25.5-cm axial field of view. After a transmission scan using a ^{137}Cs point source, a 1-minute IV bolus injection of ^{18}F-DPA-714 initiated the 90-minute emission scan. Images were reconstructed using the 3D ordinary Poisson-ordered subset expectation maximization algorithm. An additional smoothing filter implementing the point spread function was performed on the reconstructed images to achieve an intraslice spatial resolution of ~2.5 mm full width at half maximum. The resulting dynamic PET images consisted of six 1-minute frames for the initial 6 minutes (6×1), followed by 7×2- and 14×5-minute frames, with a voxel size of $1.22 \times 1.22 \times 1.22$ mm^3.

Postprocessing

In patients with MS and presymptomatic MS, white matter (WM) lesions were contoured on T2-weighted images with reference to FLAIR images using Jim (v6.0, xinapse.com/). Binary lesion masks were aligned to 3D-T1 scans with

Table 1 List of Primary Antibodies Used for Immunostaining

Target (abbreviated name)	Target (full name)	Type of primary antibody	Laboratory	Primary antibody reference	Buffer	Dilution	Time of exposure
CD163	Acute phase–regulated transmembrane protein on monocytes	Monoclonal (mouse)	Cell Marque®	MRQ-26	CC1®	1:50	32 min
CD20	Transmembrane protein expressed on B cells	Monoclonal (mouse)	Dako®	L26	CC1®	1:100	32 min
CD3	Epsilon chain of the human CD3	Monoclonal (rabbit)	Ventana®	2GV6	CC1® 30 min at 95°C	Prediluted	32 min
CD68	Lysosomal fraction of human macrophages	Monoclonal (mouse)	Dako®	KP1	CC1®	1:100	20 min
TSPO/PBR	Synthetic peptide peripheral-type benzodiazepine receptor	Monoclonal (rabbit)	Abcam®	EPR5384	CC1®	1:10,000	36 min

Abbreviation: CC1 = high pH (=8) Cell Conditioning Buffer 1 (supplied by Ventana Medical); PBR = peripheral-type benzodiazepine receptor; TSPO = translocator protein.

FMRIB's Linear Image Registration Tool (FLIRT, v5.0.9, fsl.fmrib.ox.ac.uk/),[15] followed by lesion filling. FreeSurfer (v6.0, surfer.nmr.mgh.harvard.edu/)[16] was then used on the 3D-T1 to estimate total intracranial volume (TIV) and to segment gray matter, WM, and CSF, with manual corrections when necessary.

The CPs of the lateral ventricles were manually segmented by trained neurologists on the 3 planes of the 3D-T1 using ITK-SNAP (v3.8.0, itksnap.org/) (Figure 1A),[17] and their volume was calculated. Ventricles, whole brain, cortex, and WM were extracted as additional regions of interest (ROIs) from T1-w scans using FreeSurfer.[16] In patients with MS and pre-symptomatic MS, 2 other ROIs were selected: (1) T2-w lesions and (2) normal-appearing WM (NAWM), defined as the WM without T2-weighted lesions. Volumes were divided by TIV to obtain the corresponding normalized value.

From PET scans, reconstructed dynamic data were realigned for motion correction using Statistical Parametric Mapping (SPM, v8, fil.ion.ucl.ac.uk/spm/). In particular, the first PET frame was excluded because it did not contain enough spatial information to be correctly aligned. Motion correction was performed with a 2-step procedure: all frames were first aligned to the second frame through a rigid transformation and were then registered to the mean of the frames obtained after the first realignment. Voxel-wise ^{18}F-DPA-714 distribution volume ratio (DVR) parametric maps, reflecting parenchymal ^{18}F-DPA-714 uptake, were obtained using the Logan graphical method based on the reference region.[18] Cortical, WM (NAWM), and T2-w lesion ROIs were then aligned to the corresponding DVR maps using FLIRT[14] to extract mean DVR values. CP ^{18}F-DPA-714 uptake was defined as the average standardized uptake value (SUV) inside the CPs. The use of the SUV instead of DVR at this level relies on the fact that the assumptions for Logan graphical analysis were not respected in this case. SUV maps of ^{18}F-DPA-714 were calculated from the frames between 60 and 90 minutes of acquisition (SUV$_{60-90}$) as the radioactivity concentration divided by injected dose per body mass. The mean ^{18}F-DPA-714 SUV$_{60-90}$ in the CPs was extracted for each patient by overlapping the CP masks to the SUV maps, after performing CP partial volume correction with the single target correction method in PET partial volume correction software (PETPVC, v1.2.0-b, github.com/UCL/PETPVC).[4,19]

Postmortem Analysis

CP postmortem samples were obtained from the French National BrainBank Donation Program Neuro-CEB. Samples were obtained from 3 patients with MS with severe disease (2 males, 1 secondary progressive/2 primary progressive, age: 54 ± 11 years, disease duration: 29 ± 10 years) and 2 non-MS controls (2 males, 1 epilepsy and 1 HC, age: 63 ± 10 years). Half of the brain was fixed by immersion in 4% formaldehyde; formalin-fixed samples were embedded in paraffin and cut at a 3-μm thickness. Selected sections were immunostained using a Ventana BenchMark stainer (Roche, Tucson, AZ). Diaminobenzidine and alkaline phosphatase were used as chromogens. Pretreatment and antibodies used for immunostaining are listed in Table 1.

Statistical Analysis

STATA (v14.0, stata.com/) and R (R-project.org/) were used, considering 2-sided $p < 0.05$ as significant.

The sample size estimated for showing a CP enlargement in RIS was calculated based on an expected 25% increase (inferior to the 35% found in patients in our previous study)[4] in mean CP volume compared with HCs. Setting statistical power to 80%, significance level (alpha) to 0.05, and enrollment ratio between MS and HCs to 1:2, a minimum of 20 patients with presymptomatic MS was necessary to detect a ≥25% intergroup difference in CP volume.

Wilcoxon-Mann-Whitney and Fisher tests were used as appropriate for age and sex differences. A Shapiro-Wilk normality test was performed to check the distribution of volumetric data.

Table 2 Comparison of Volumes of Different Brain Regions Between Presymptomatic MS, MS, and HCs

Volume	Presymptomatic MS	MS	HCs	Presymptomatic MS vs MS	Presymptomatic MS vs HCs
TIV	$15.3 \pm 1.9 \times 10^5$	$14.9 \pm 1.5 \times 10^5$	$14.7 \pm 1.6 \times 10^5$	$p = 0.27$	$p = 0.21$
Brain parenchyma	0.7 ± 0.07	0.6 ± 0.04	0.7 ± 0.08	$p < 0.001$	$p = 0.11$
Ventricles	$16.4 \pm 7.1 \times 10^{-3}$	$20.4 \pm 8.2 \times 10^{-3}$	$12.9 \pm 4.7 \times 10^{-3}$	$p = 0.03$	$p = 0.009$
Choroid plexus	$14.9 \pm 5.2 \times 10^{-4}$	$15.9 \pm 4.5 \times 10^{-4}$	$11.3 \pm 3.9 \times 10^{-4}$	$p = 0.35$	$p < 0.001$

Abbreviations: HCs = healthy controls; MS = multiple sclerosis; TIV = total intracranial volume.
Volumes were normalized on total intracranial volume (except for the first row) and expressed as mean ± SD. Mean comparison between groups was performed using unpaired t tests after the normality test (Shapiro-Wilk). p = p value from the t test.

Intergroup differences in CP volume, ventricular volume, brain parenchymal volume, and TIV were assessed through unpaired t tests. Pearson's r was used for the correlation between CP and ventricular volume in patients with presymptomatic MS. Multivariable linear regression models adjusted for age and sex were used to test differences in ventricular volume, whole brain parenchymal volume, and TIV (dependent variables) between presymptomatic MS and MS or HCs (independent binary variables). The same models, additionally adjusted for ventricular and whole brain parenchymal volume, were fitted to test differences in TIV-normalized CP volume: (1) between presymptomatic MS and MS or HCs; (2) within presymptomatic MS, between CSF-positive vs CSF-negative patients, and between converters to MS vs nonconverters (additionally accounting for the follow-up length).

In the subgroup analysis on the PET cohort, differences in age, CP volume, mean ^{18}F-DPA-714 DVR, and CP ^{18}F-DPA-714 SUV_{60-90} between the presymptomatic case and MS or HCs were assessed through Crawford-Howell tests.

Data Availability

Anonymized data are available on reasonable request from any qualified investigator.

Results

CPs Are Larger in Patients With Presymptomatic MS

The presymptomatic group (n = 27) was not different from MS and HCs in mean age (years, presymptomatic MS: 42 ± 11, MS: 42 ± 12, HCs: 42 ± 14.4, $p = 0.72$ and $p = 0.73$, respectively) or sex (women, presymptomatic MS: 17, MS: 49, HCs: 28, $p = 0.20$ and $p = 0.48$, respectively). Lumbar puncture was performed in 24 patients with presymptomatic MS, of which 11 had positive CSF (either high IgG index or positive oligoclonal bands; 46%). The median follow-up from the analyzed MRI scan was 30 (7–95) months. Conversion to MS occurred in 5 patients (18.5%).

When assessing volumetric differences between the presymptomatic MS cohort and either MS or HCs, mean CP volume was 32% higher in the presymptomatic MS group vs HCs (presymptomatic MS, mean normalized CP volume ± SD: $14.9 \pm 5.2 \times 10^{-4}$, HCs, mean normalized CP volume ± SD: $11.3 \pm 3.9 \times 10^{-4}$, $p < 0.001$). On the contrary, there was no difference in CP volume between presymptomatic MS and MS (MS, mean normalized CP volume ± SD: $15.9 \pm 4.5 \times 10^{-4}$, $p = 0.35$) (Figure 1B). A significant difference between the presymptomatic MS group and HCs was also found in ventricular size (presymptomatic MS, mean normalized ventricular volume ± SD: $16.4 \pm 7.1 \times 10^{-3}$, HCs, mean normalized ventricular volume ± SD: $12.9 \pm 4.7 \times 10^{-3}$, $p = 0.009$), but not in TIV or brain parenchymal volume (Table 2). In the presymptomatic cohort, CP volume correlated with ventricular volume (r = 0.55, $p = 0.003$), as already described for MS.[4] After adjusting for the ventricular size, CPs were still larger in RIS than HCs (β = 0.38, regression coefficient = 3.76×10^{-4}, 95% CI = 1.54×10^{-4}:5.98×10^{-4}, $p = 0.001$). There was no statistical difference in the CP volume adjusted for ventricular size between RIS and MS ($p = 0.69$). In the presymptomatic MS cohort, CP volume in patients with a CSF-positive pattern (defined as either high IgG index or positive oligoclonal bands, n = 11) was similar (mean normalized CP volume ± SD: $13.1 \pm 3.7 \times 10^{-4}$), compared with patients with a CSF-negative pattern (n = 13, mean normalized CP volume ± SD: $16.7 \pm 6.5 \times 10^{-4}$, $p = 0.20$). Mean CP size did not significantly differ between patients with RIS who converted to MS during follow-up (n = 5, mean normalized CP volume ± SD: $16.1 \pm 3.8 \times 10^{-4}$) and those who did not convert (n = 22, mean normalized CP volume ± SD: $14.7 \pm 5.5 \times 10^{-4}$, $p = 0.74$).

Higher CP DPA Uptake in a Single Presymptomatic Patient

The woman with presymptomatic MS who underwent both MRI and PET had 2 WM hyperintensities (periventricular and deep WM) on baseline MRI, allowing to classify her as presymptomatic MS. Eight months later, she experienced a first clinical event, together with the appearance of a new gadolinium-positive lesion located in the left frontal WM and a new gadolinium-negative lesion in the right juxta cortical WM, leading to the diagnosis of MS according to the McDonald criteria 2010. At baseline, she did not differ from MS or HC for age ($p = 0.08$ and $p = 0.1$). Her CP volume was 77% larger than the mean volume measured in HCs (Figure 1C, the case's normalized CP volume: 20×10^{-4}, $p =$

Figure 2 Higher ^{18}F-DPA-714 Uptake in the CPs of Presymptomatic MS
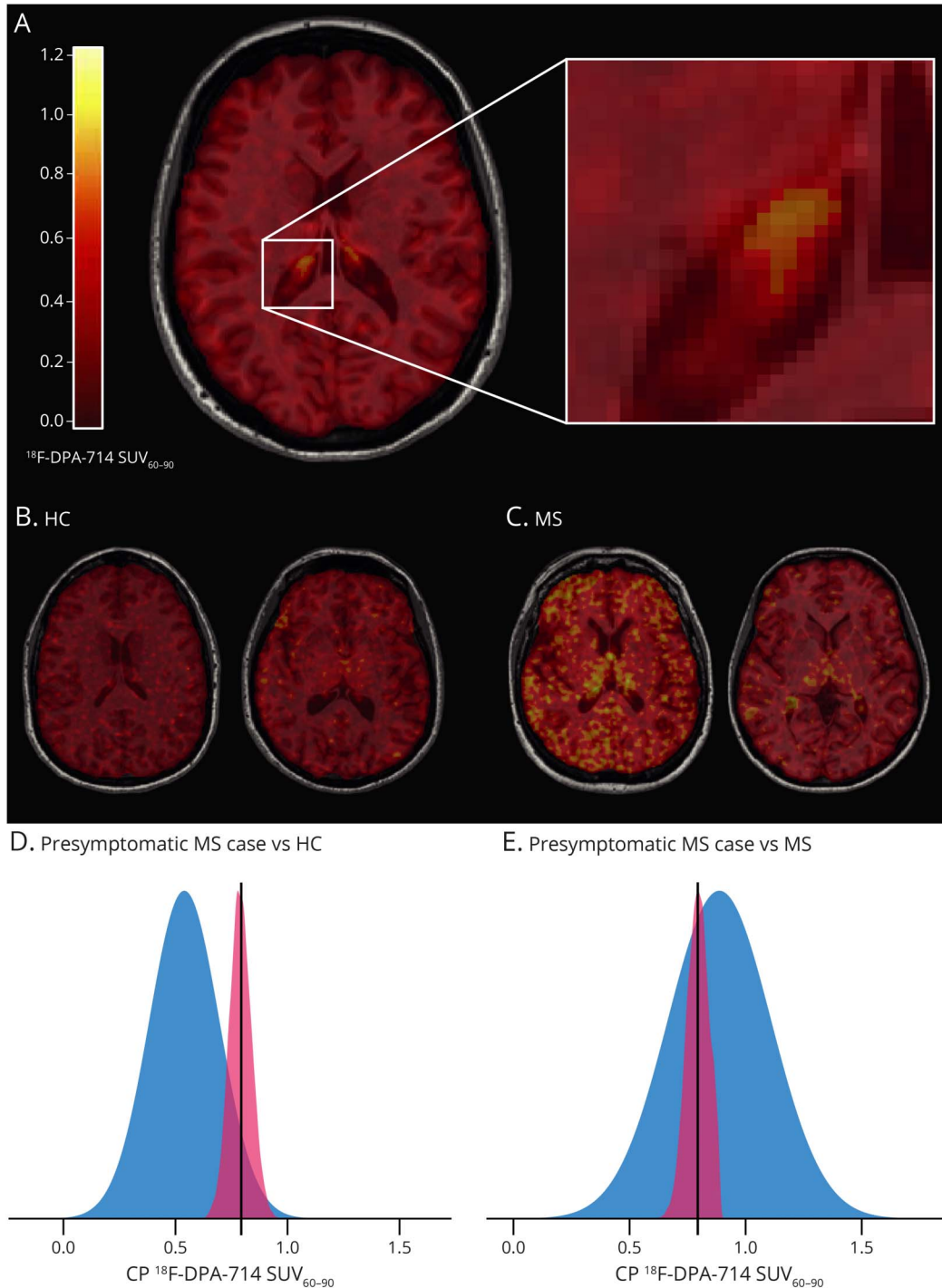

(A) Axial ^{18}F-DPA-714 SUV$_{60-90}$ map registered onto the 3D T1-weighted magnetization-prepared rapid gradient echo (MPRAGE) image of the presymptomatic MS case, with the corresponding color bar (left) and magnification on the CP of the right lateral ventricle (right). (B, C) Examples of axial ^{18}F-DPA-714 SUV$_{60-90}$ maps registered onto the 3D T1-weighted MPRAGE images from 2 controls (B) and 2 patients with RRMS (C). (D, E) Graphical illustration of the distribution of CP ^{18}F-DPA-714 SUV$_{60-90}$ in HCs vs the presymptomatic woman (D) and in MS vs the presymptomatic woman (E) from the Crawford-Howell test. The presence of a distribution for a single case value is based on the assumptions of the test performed and depends on the statistics of the reference cohort. CP = choroid plexus; HCs = healthy controls; MS = multiple sclerosis; SUV$_{60-90}$ = standardized uptake value between 60 and 90 minutes of acquisition; TIV = total intracranial volume.

0.008), being greater than the one measured in 98.4% of HCs (95% CI = 9.16×10^{-4}:0.04) and similar to the mean volume of patients with MS ($p = 0.09$) (Figure 1D). Looking at TSPO PET (Figure 2A), her ^{18}F-DPA-714 SUV$_{60-90}$ within CPs was 33% higher than that in HCs (the case's CP SUV$_{60-90}$: 0.794, mean CP SUV$_{60-90}$ ± SD of HCs: 0.596 ± 0.13, $p = 0.04$), being greater than the one measured in 92% of HCs (95% CI = 6.35×10^{-3}:0.17) (Figure 2, B and D), but did not differ

Figure 3 TSPO+/CD163+ Macrophages Are Found in MS CPs
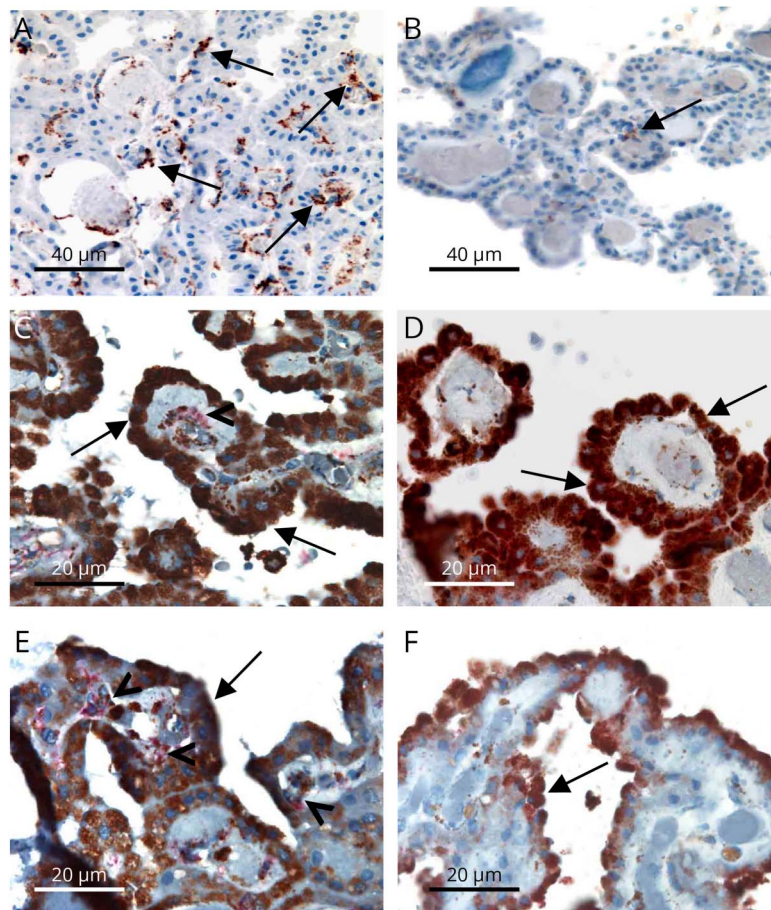
(A, B) Excess of CD163^{+} macrophages (mouse monoclonal antibody, Cell Marque®; brown, arrows) in a PPMS case (A) compared with a healthy control (B). (C, F) TSPO (monoclonal rabbit antibody, Abcam®; brown) is highly expressed in epithelial cells (arrows) of choroid plexuses in both MS (C: PPMS and E: SPMS) and controls (D: HCs and F: epilepsy control). CD163^{+} (red) and TSPO^{+} (brown) perivascular macrophages (arrowheads) are found in MS (C, E), but not in controls (D, F). Scale bars = 40 μm (A, B) and 20 μm (C–F). HCs = healthy controls; MS = multiple sclerosis; PPMS = primary progressive MS; SPMS = secondary progressive MS; TSPO = translocator protein.

from the CP SUV_{60-90} of the MS group (mean CP SUV_{60-90} ± SD of MS: 0.887 ± 0.22, p = 0.17) (Figure 2, C and E). No significant differences between the presymptomatic MS and HCs were found for ^{18}F-DPA-714 DVR in the cortex (the case's cortex DVR: 1.41, mean cortex DVR ± SD of HCs: 1.32 ± 0.13, p = 0.13), in the WM (the case's WM DVR: 0.96, mean WM DVR ± SD of HCs: 0.89 ± 0.08, p = 0.10), or in T2-w hyperintensities compared with HCs' WM (the case's DVR in T2-w hyperintensities: 0.98, p = 0.07).

TSPO Is Expressed by Epithelial Cells and CD163^{+} Macrophages in the CPs of Patients With MS

In CPs of patients with a history of active MS and non-MS controls, a high TSPO expression was found in epithelial cells. CPs of patients with MS also showed an excess of CD163^{+} macrophages compared with controls (Figure 3, A and B). Double immunostaining identified a TSPO^{+} pool that was also positive for the monocyte/macrophage-specific marker CD163 in MS alone (Figure 3, C–F). No cells coexpressing TSPO with the T-lymphocyte marker CD3, the B-lymphocyte marker CD20, or the peripheral macrophage marker CD68 were identified.

Discussion

We investigated the imaging signature of CPs at the preclinical stage of MS vs HCs through a combination of MRI and ^{18}F-DPA-714 TSPO-PET. We provide evidence that CPs are larger (32% increase) and have higher ^{18}F-DPA-714 uptake (33% increase in the single patient included in the analysis) in presymptomatic patients compared with HCs. CP histology from patients with MS and non-MS controls showed a population of CD163^{+}/TSPO^{+} macrophages, detected only in MS, which may contribute, at least partly, to the difference in TSPO expression between the 2 conditions.

Beyond CSF production, CPs regulate immune cell trafficking between the blood and the CNS, involving CP mononuclear phagocytes in this complex homeostasis.[20,21] In MS, the neuroinflammatory component is not currently detected by clinical MRI but can be quantified using PET with TSPO tracers such as ^{18}F-DPA-714.[22] We recently described in vivo a higher CP ^{18}F-DPA-714 uptake in MS vs controls, this difference being particularly pronounced in RRMS.[4] Here, we extend this finding by showing similar changes in the CPs of preclinical MS, suggesting that a BCSFB deregulation could

be among the earliest processes characterizing MS pathophysiology. Of note, only CPs, but not the brain parenchyma, showed increased ^{18}F-DPA-714 binding in the presymptomatic patient, mimicking the sequence of events characterizing EAE, in which inflammation within CPs precedes the parenchymal infiltrate and demyelination.[6] Neuropathology has described an increased density of antigen-presenting cells, leukocyte infiltration, and overexpression of proinflammatory adhesion molecules in MS CPs.[23,24] In the postmortem analysis of CPs from patients with a previous severe course of the disease and from controls, we observed, as expected, that TSPO was expressed by epithelial and vascular cells in all patients,[25] but an additional expression by CD163^{+} macrophages selectively characterized MS, this difference potentially explaining their higher ^{18}F-DPA-714 uptake. Of interest, this TSPO expression was restricted to CD163^{+} cells and was not detected on CD3^{+} or CD20[+-] lymphocytes nor on CD68^{+} monocytes, suggesting a selective increase in perivascular CP macrophages involved in antigen presentation in MS.[20,26] Unfortunately, lacking pathologic samples, it was not possible to explore whether similar alterations also occur at the earliest MS stages, and a more heterogeneous TSPO expression by distinct subsets of monocytes in this phase cannot be excluded. In the case reported here, a first relapse occurred few months after the PET evidence of inflamed CPs, and future studies applying TSPO-PET at the preclinical stage will be of outstanding interest to decipher whether the inflammatory status of CPs could be predictive of conversion toward defined MS.

We previously demonstrated a correlation between ^{18}F-DPA-714 uptake in the CPs and their increased volume on MRI in RRMS,[4] arguing for the possibility to use CP enlargement as a proxy of CP inflammation. A recent study has further reinforced the relationship between CP enlargement, their inflammatory status, and parenchymal inflammation.[5] Taken together, these results attest that CP volumetric analysis could represent a promising in vivo biomarker of MS neuroinflammation.[5] In accordance with this hypothesis, CP enlargement in presymptomatic MS confirms that this imaging signature is an early phenomenon along the disease course. Whether CP imaging modifications are stable or fluctuate with the inflammatory phases of the disease remains to be addressed. Focusing on RIS may offer complementary assets to (1) disentangle the temporal, and possibly causal, relationship between CP alterations and symptom onset; (2) follow the natural history of CP modifications without the bias of treatment and estimate the potential impact of disease-modifying therapies, once these are introduced at the defined MS stage; and (3) characterize the involvement of CPs in the physiopathology of lesion formation and fate, investigating the initial inflammatory infiltration into the CNS, the BCSFB disruption, and the relationship with CSF inflammatory markers.

Another important question to be addressed is to what extent CP volumetric and inflammatory alterations are specific for MS with respect to other acute or chronic inflammatory/infectious disorders of the CNS. This goes beyond the scopes of this study, but very recent findings suggest that CP enlargement is detected in MS in contrast to optic neuromyelitis,[27] pointing at a possible specificity of CP modifications in relation to the respective pathogenesis.

Given the low cost and higher accessibility of MRI,[28] CP volumetric analysis could become an easy technique to assess this imaging signature on a larger scale. To this aim, the development of artificial intelligence–based methods for automatic CP segmentation[29,30] and the integration of additional MRI sequences for perfusion[31] could allow a time- and cost-sparing evaluation of CP modifications, compared with PET.

This study has potential limitations. The RIS group was collected in a clinical setting, producing heterogeneity of MRI scanners and parameter acquisitions. Nonetheless, the ability to identify CP volume differences even in the real world prompts for the possible application of this metric outside of standard research protocols. In addition, the presymptomatic cohort, despite being large enough to detect intergroup differences, was relatively small. This may have affected the absence of detectable CP volume differences between CSF-positive and CSF-negative patients or converters to MS vs nonconverters, given the low proportion of people who developed MS over time.[10] Therefore, studies on larger populations and longer follow-up periods are necessary to better define the impact of CP modifications on disease conversion. Another limitation concerns the postmortem data presented here. The similar ^{18}F-DPA-714 PET changes found in the CPs of the presymptomatic patient and of patients with more advanced MS may suggest that they had an identical underlying pathologic substrate, but we lacked a direct postmortem analysis of CPs at the RIS stage to formally demonstrate this. Of note, however, among early, newly diagnosed patients with MS, an involvement of a CD163-positive macrophage/microglial population was described,[32] echoing what found in more advanced stages,[33] supporting the hypothesis of an early contribution of this macrophage population at the RIS stage.

To note, our histology data show that epithelial cells are a major source of TSPO expression in the CPs, and we have not quantified the relative contribution of epithelial and macrophage cells to TSPO overexpression in MS CPs vs non-MS controls. Therefore, it is possible that, beyond CD163^{+}/TSPO^{+} macrophages, an expanded TSPO-positive epithelial compartment in MS contributes to the higher ^{18}F-DPA-714 uptake in MS. Finally, regarding the PET part of the study, we highlight that the comparison in terms of ^{18}F-DPA-714 uptake was made between only 1 presymptomatic patient (n = 1) and a group of patients with MS (n = 22) or HCs (n = 19); hence, these data need further confirmation on a PET cohort of presymptomatic patients.

In conclusion, by identifying an imaging signature in CPs already in presymptomatic MS, our work supports their role

from the early phases of disease development and encourages further investigations on the involvement of CP immune infiltration and BCSFB dysfunction in disease onset.

Study Funding

Disclosure

Publication History

Appendix Authors

Name	Location	Contribution
Vito A.G. Ricigliano, MD, PhD	Sorbonne Université, Paris Brain Institute, ICM, CNRS, Inserm, Paris, France; Neurology Department, St Antoine Hospital, APHP-Sorbonne, Paris, France	Drafting/revision of the manuscript for content, including medical writing for content; study concept or design; and analysis or interpretation of data

Appendix (continued)

Name	Location	Contribution
Céline Louapre, MD, PhD	Sorbonne Université, Paris Brain Institute, ICM, CNRS, Inserm, Paris, France; Neurology Department, Pitié-Salpêtrière Hospital, APHP-Sorbonne, Paris, France	Major role in the acquisition of data
Emilie Poirion, PhD	Sorbonne Université, Paris Brain Institute, ICM, CNRS, Inserm, Paris, France; Service d'Imagerie Médicale, Hôpital Fondation Adolphe de Rothschild, Paris, France	Analysis or interpretation of data
Annalisa Colombi, MD	Sorbonne Université, Paris Brain Institute, ICM, CNRS, Inserm, Paris, France	Analysis or interpretation of data
Arya Yazdan Panah, MSc	Sorbonne Université, Paris Brain Institute, ICM, CNRS, Inserm, Paris, France	Analysis or interpretation of data
Andrea Lazzarotto, MD	Sorbonne Université, Paris Brain Institute, ICM, CNRS, Inserm, Paris, France; Neurology Department, St Antoine Hospital, APHP-Sorbonne, Paris, France	Analysis or interpretation of data
Emanuele Morena, MD	Sorbonne Université, Paris Brain Institute, ICM, CNRS, Inserm, Paris, France	Analysis or interpretation of data
Elodie Martin, PhD	Sorbonne Université, Paris Brain Institute, ICM, CNRS, Inserm, Paris, France	Analysis or interpretation of data
Michel Bottlaender, MD, PhD	Université Paris-Saclay, CEA, CNRS, Inserm, BioMaps, Service Hospitalier Frédéric Joliot, Orsay, France	Major role in the acquisition of data
Benedetta Bodini, MD, PhD	Sorbonne Université, Paris Brain Institute, ICM, CNRS, Inserm, Paris, France; Neurology Department, St Antoine Hospital, APHP-Sorbonne, Paris, France	Major role in the acquisition of data
Danielle Seilhean, MD	Sorbonne Université, Paris Brain Institute, ICM, CNRS, Inserm, Paris, France; Neuropathology Department, Pitié-Salpêtrière Hospital, APHP-Sorbonne, Paris, France	Drafting/revision of the manuscript for content, including medical writing for content; major role in the acquisition of data; and analysis or interpretation of data
Bruno Stankoff, MD, PhD	Sorbonne Université, Paris Brain Institute, ICM, CNRS, Inserm, Paris, France; Neurology Department, St Antoine Hospital, APHP-Sorbonne, Paris, France	Drafting/revision of the manuscript for content, including medical writing for content; major role in the acquisition of data; study concept or design; and analysis or interpretation of data

References

1. Khasawneh AH, Garling RJ, Harris CA. Cerebrospinal fluid circulation: what do we know and how do we know it? *Brain Circ.* 2018;4(1):14-18.
2. Ghersi-Egea JF, Strazielle N, Catala M, Silva-Vargas V, Doetsch F, Engelhardt B. Molecular anatomy and functions of the choroidal blood-cerebrospinal fluid barrier in health and disease. *Acta Neuropathol.* 2018;135(3):337-361.
3. Johanson CE, Stopa EG, McMillan PN. The blood-cerebrospinal fluid barrier: structure and functional significance. *Methods Mol Biol.* 2011;686:101-131.

4. Ricigliano VAG, Morena E, Colombi A, et al. Choroid plexus enlargement in inflammatory multiple sclerosis: 3.0-T MRI and translocator protein PET evaluation. *Radiology.* 2021;301(1):166-177.

5. Fleischer V, Gonzalez-Escamilla G, Ciolac D, et al. Translational value of choroid plexus imaging for tracking neuroinflammation in mice and humans. *Proc Natl Acad Sci U S A.* 2021;118(36):e2025000118.

6. Reboldi A, Coisne C, Baumjohann D, et al. C-C chemokine receptor 6-regulated entry of TH-17 cells into the CNS through the choroid plexus is required for the initiation of EAE. *Nat Immunol.* 2009;10(5):514-523.

7. Schmitt C, Strazielle N, Ghersi-Egea JF. Brain leukocyte infiltration initiated by peripheral inflammation or experimental autoimmune encephalomyelitis occurs through pathways connected to the CSF-filled compartments of the forebrain and midbrain. *J Neuroinflammation.* 2012;9:187.

8. Okuda DT, Mowry EM, Beheshtian A, et al. Incidental MRI anomalies suggestive of multiple sclerosis: the radiologically isolated syndrome. *Neurology.* 2009;72(9):800-805.

9. De Stefano N, Giorgio A, Tintoré M, et al, MAGNIMS Study Group. Radiologically isolated syndrome or subclinical multiple sclerosis: MAGNIMS consensus recommendations. *Mult Scler.* 2018;24(2):214-221.

10. Okuda DT, Siva A, Kantarci O, et al. Radiologically isolated syndrome: 5-year risk for an initial clinical event. *PLoS One.* 2014;9(3):e90509.

11. Lebrun-Frénay C, Rollot F, Mondot L, et al, RISC, SFSEP, and OFSEP Investigators. Risk factors and time to clinical symptoms of multiple sclerosis among patients with radiologically isolated syndrome. *JAMA Netw Open.* 2021;4(10):e2128271.

12. Bodini B, Poirion E, Tonietto M, et al. Individual mapping of innate immune cell activation is a candidate marker of patient-specific trajectories of worsening disability in multiple sclerosis. *J Nucl Med.* 2020;61(7):1043-1049.

13. Owen DRJ, Gunn RN, Rabiner EA, et al. Mixed-affinity binding in humans with 18-kDa translocator protein ligands. *J Nucl Med.* 2011;52(1):24-32.

14. Lavisse S, Goutal S, Wimberley C, et al. Increased microglial activation in patients with Parkinson disease using [18 F]-DPA-714 TSPO PET imaging. *Parkinsonism Relat Disord.* 2021;82:29-36.

15. Jenkinson M, Smith S. A global optimisation method for robust affine registration of brain images. *Med Image Anal.* 2001;5(2):143-156.

16. Fischl B, Salat DH, Busa E, et al. Whole brain segmentation: automated labeling of neuroanatomical structures in the human brain. *Neuron.* 2002;33(3):341-355.

17. Yushkevich PA, Piven J, Hazlett HC, et al. User-guided 3D active contour segmentation of anatomical structures: significantly improved efficiency and reliability. *Neuroimage.* 2006;31(3):1116-1128.

18. García-Lorenzo D, Lavisse S, Leroy C, et al. Validation of an automatic reference region extraction for the quantification of [18F]DPA-714 in dynamic brain PET studies. *J Cereb Blood Flow Metab.* 2018;38(2):333-346.

19. Thomas BA, Cuplov V, Bousse A, et al. PETPVC: a toolbox for performing partial volume correction techniques in positron emission tomography. *Phys Med Biol.* 2016;61(22):7975-7993.

20. Ivan DC, Walthert S, Berve K, Steudler J, Locatelli G. Dwellers and trespassers: mononuclear phagocytes at the borders of the central nervous system. *Front Immunol.* 2020;11:609921.

21. Bogie JFJ, Stinissen P, Hendriks JJA. Macrophage subsets and microglia in multiple sclerosis. *Acta Neuropathol.* 2014;128(2):191-213.

22. Bodini B, Tonietto M, Airas L, Stankoff B. Positron emission tomography in multiple sclerosis–straight to the target. *Nat Rev Neurol.* 2021;17(11):663-675.

23. Rodríguez-Lorenzo S, Konings J, Van Der Pol S, et al. Inflammation of the choroid plexus in progressive multiple sclerosis: accumulation of granulocytes and T cells. *Acta Neuropathol Commun.* 2020;8(1):9.

24. Vercellino M, Votta B, Condello C, et al. Involvement of the choroid plexus in multiple sclerosis autoimmune inflammation: a neuropathological study. *J Neuroimmunol.* 2008;199(1-2):133-141.

25. Betlazar C, Harrison-Brown M, Middleton RJ, Banati R, Liu G-J. Cellular sources and regional variations in the expression of the neuroinflammatory marker translocator protein (TSPO) in the normal brain. *Int J Mol Sci.* 2018;19(9):2707.

26. McMenamin PG, Wealthall RJ, Deverall M, Cooper SJ, Griffin B. Macrophages and dendritic cells in the rat meninges and choroid plexus: three-dimensional localisation by environmental scanning electron microscopy and confocal microscopy. *Cell Tissue Res.* 2003;313(3):259-269.

27. Müller J, Sinnecker t, Wendebourg MJ, et al. Choroid plexus volume in multiple sclerosis vs neuromyelitis optica spectrum disorder: a retrospective, cross-sectional analysis. *Neurol Neuroimmunol Neuroinflamm.* 2022;9(3):e1147.

28. Niccolini F, Su P, Politis M. PET in multiple sclerosis. *Clin Nucl Med.* 2015;40(1):e46-52.

29. Akkus Z, Galimzianova A, Hoogi A, Rubin DL, Erickson BJ. Deep learning for brain MRI segmentation: state of the art and future directions. *J Digit Imaging.* 2017;30(4):449-459.

30. Schmidt-Mengin M, Ricigliano VAG, Bodini B, et al. Axial multi-layer perceptron architecture for automatic segmentation of choroid plexus in multiple sclerosis. In: Colliot O, Işgum I, eds. *Proc SPIE.* 2022;12032:44-53.

31. Zhao L, Taso M, Dai W, Press DZ, Alsop DC. Non-invasive measurement of choroid plexus apparent blood flow with arterial spin labeling. *Fluids Barriers CNS.* 2020;17(1):58.

32. Stilund M, Reuschlein A-K, Christensen T, Moller HJ, Rasmussen PV, Petersen T. Soluble CD163 as a marker of macrophage activity in newly diagnosed patients with multiple sclerosis. *PLoS One.* 2014;9(6):e98588.

33. Zhang Z, Zhang Z-Y, Schittenhelm J, Wu Y, Meyermann R, Schluesener HJ. Parenchymal accumulation of CD163+ macrophages/microglia in multiple sclerosis brains. *J Neuroimmunol.* 2011;237(1-2):73-79.